Available online at www.sciencedirect.com
ScienceDirect
Sensors and Actuators A 141 (2008) 603–609
SENSORS AND ACTUATORS A PHYSICAL
www.elsevier.com/locate/sna

Minimum scale controlled topology optimization and experimental test of a micro thermal actuator

Seok Heo [a], Gil Ho Yoon [b], Yoon Young Kim [a,*]

[a] *National Creative Research Initiatives Center for Multiscale Design, Institute of the Advanced Machinery Design and School of Mechanical and Aerospace Engineering, Seoul National University, Sillim-dong San 56-1, Kwanak-gu, Seoul 151-742, Republic of Korea*
[b] *Department of Mechanical Engineering, Solid Mechanics, The Technical University of Denmark, Nils Koppels Allé 404, DK-2800 Lyngby, Denmark*

Received 16 January 2007; received in revised form 30 September 2007; accepted 2 October 2007
Available online 9 October 2007

Abstract

This paper is concerned with the optimal topology design, fabrication and test of a micro thermal actuator. Because the minimum scale was controlled during the design optimization process, the production yield rate of the actuator was improved considerably; alternatively, the optimization design without scale control resulted in a very low yield rate. Using the minimum scale controlling topology design method developed earlier by the authors, micro thermal actuators were designed and fabricated through a MEMS process. Moreover, both their performance and production yield were experimentally tested. The test showed that control over the minimum length scale in the design process greatly improves the yield rate and reduces the performance deviation.

Keywords: Micro thermal actuator; Design; Minimum scale control; Topology optimization

1. Introduction

The objective of this research is to design a micro thermal actuator by a topology optimization method and to fabricate it for experimental test. Because micro thermal actuators are used in many applications [1–6], the design optimization of such actuators is an important issue. If actuation performance was the only design issue, the straightforward application of the topology optimization method would be perhaps the best approach. However, the method that did not consider production yield may not be useful for practical applications. Therefore, a design optimization method incorporating the production yield issue needs to be considered and tested experimentally for its actual performance. Recently, a topology optimization method embedded with a minimum length scale controlling strategy has been developed by the authors [7] to consider actuator performance and the minimum length scale during the optimization process. The minimum length scale control is an indirect means to consider production yield. In this investigation, we will fabricate actuators by using the method of [7] and investigate experimentally the actual performance and yield rate of the actuators. With this study, the importance of the minimum length scale control during design process will be shown and the practical usefulness of the design method will be tested.

Although design optimization methods are useful for MEMS devices including micro thermal actuators, the optimized performance by typical numerical methods is often difficult to realize because fabrication limitations such as constraints on minimum length scale, aspect ratio, etc., were not considered during the optimization process (see [8–11]). For example, the topology optimization method [12,13], among others, has become more attractive because it does not require any baseline design to begin with. However, the major hurdle in applying the topology optimization method in MEMS design is the difficulty to control production yield rate. The production yield rate is primarily related to the minimum length scale of the optimized layout by the topology optimization.

Fig. 1(a) shows an optimized micro thermal actuator obtained by topology optimization without controlling its minimum length scale. Fig. 1(b) shows two fabricated actuators on Silicon

* Corresponding author. Tel.: +82 2 880 7154; fax: +82 2 883 1513.
E-mail address: yykim@snu.ac.kr (Y.Y. Kim).

0924-4247/$ – see front matter © 2007 Elsevier B.V. All rights reserved.
doi:10.1016/j.sna.2007.10.003

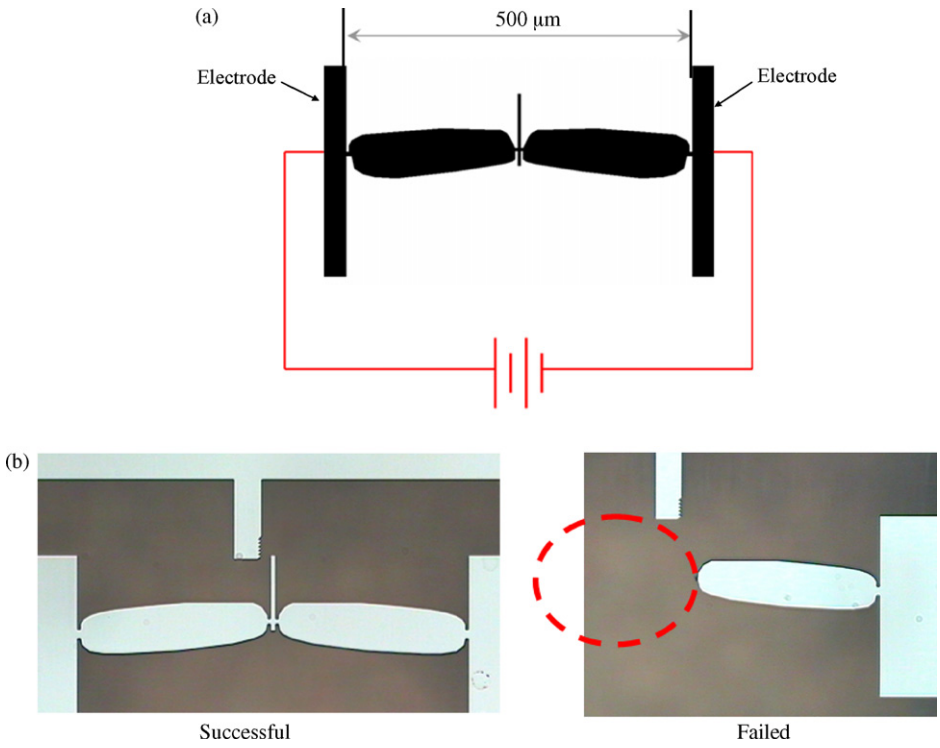

Fig. 1. A thermal actuator designed by the topology optimization without considering the minimum length scale. The design objective was to maximize the tip displacement for a given voltage input. (a) Design by the topology optimization, (b) fabricated thermal actuators at Seoul National University.

on Insulator (SOI) wafer: one was successful and the other unsuccessful. The success yield was less than 10% when the actuator in Fig. 1(a) was fabricated. The failure in Fig. 1(b) is apparently due to residual stress developed during the MEMS process, especially prevalent at the narrow thin parts of the actuator. As another failure mode, Fig. 2 shows a failed actuator due to the footing phenomenon [14]. From the failed results in Figs. 1 and 2, one can see that design optimization targeted only at performance hardly produces actuators at a high yield rate. Therefore, one needs to consider the issue of production rate either directly or indirectly in design optimization process.

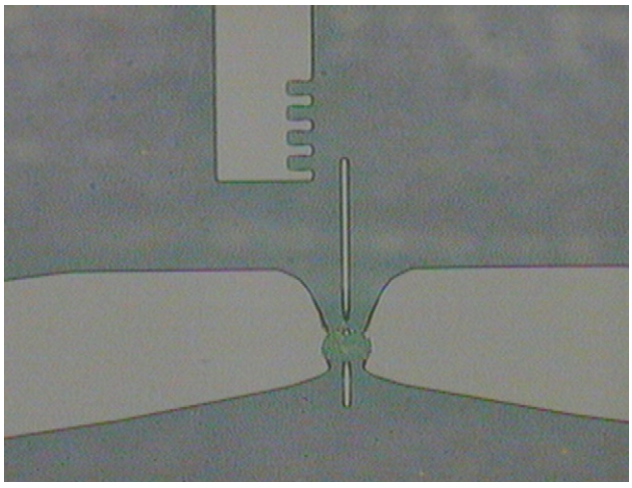

Fig. 2. Failure of a thermal actuator due to footing phenomena.

If a design optimization method can consider all MEMS design issues such as the level of residual stresses, the actuator failure rate can be substantially reduced. However, to our knowledge, no such method is yet available, so far. Thereby, an indirect approach of [7], an approach to control the minimum length scale within the topology optimization setting, can be used as an alternative.

In order to check the effectiveness of the minimum length scale controlling approach in actual MEMS design and fabrication, two approaches as described in Fig. 3 will be compared. Approach 1, a traditional approach, does not consider any scale issue in the topology design optimization step; only actuation performance is considered. The optimized design is then simply post-processed in such a way that the sizes of all members are made larger than the required minimum length ($l_{\min}$). Approach 2 carries out the topology optimization with the minimum length control. In other words, the design optimization method finds the best-performing actuator whose member size is larger than $l_{\min}$ during the optimization process. No artificial scale-related post-processing is needed in Approach 2.

This paper is organized as follows. In Section 2, a brief introduction of the topology design optimization method incorporating a minimum length scale control technique [7] is given. Section 3 presents the fabrication process of the thermal actuator and the experimental test results on performance and yield rate. The findings of this research are summarized in Section 4.

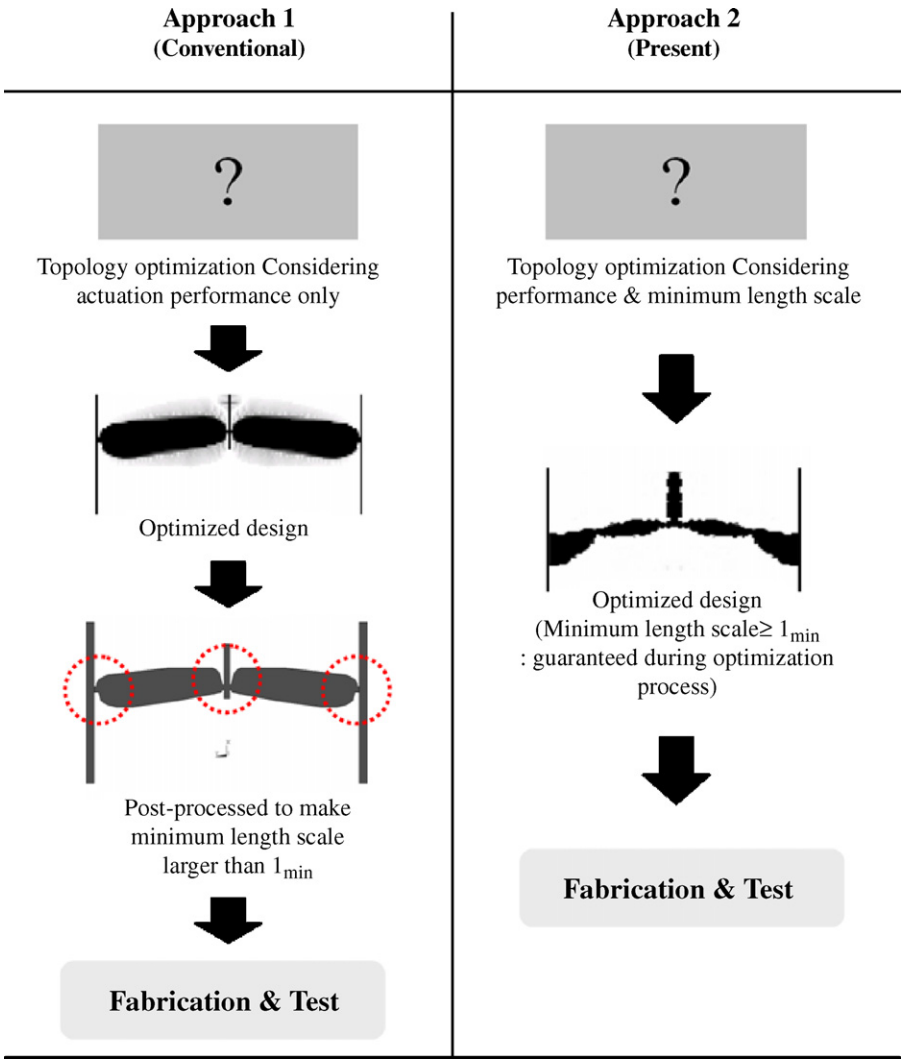

Fig. 3. Comparison of the design methods for micro thermal actuators.

2. Design of thermal actuators applying the minimum scale control method

The design problem to be considered is depicted in Fig. 4. The design domain is a 500 μm × 200 μm gray region. The design objective is to maximize the vertical displacement at the point A under a given voltage input supplied through two side electrodes. To avoid obtaining a rigid-body mechanism and to simulate the actual load at A, a spring of spring constant k_s is installed at the actuation point A. The design optimization problem can be set up as:

Maximize	u_y^A (vertical displacement of A)
Subject to	a mass constraint

To solve the topology optimization, the design domain is discretized by finite elements. An optimization algorithm is employed to obtain an optimal actuator configuration. The thermal actuator is actuated by thermal expansion from Joule's heat energy. The analysis of thermal actuators involves electric, thermal and structural phenomena. Because nonlinear phenomena

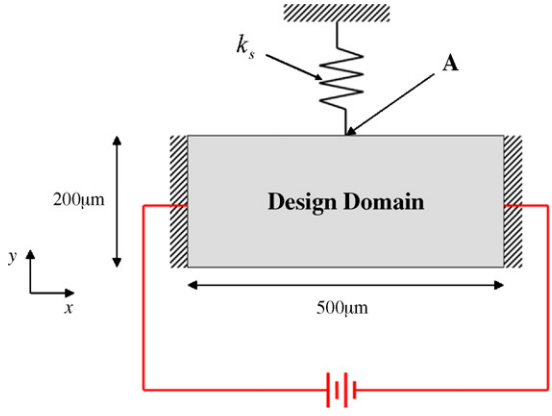

Fig. 4. The problem definition for the design of a thermal actuator (k_s = 1 N/m, Young's modulus = 165.7 GPa, Poisson's ratio = 0.22, depth = 15 μm, the electric conductivity = 10000 K(Ω m)$^{-1}$, the thermal conductivity = 150.0 W/(Km), the convection coefficient = 18.7 × 10^3 W/(m^{2}K), thermal expansion coefficient = 2.6 × 10^{-6} K^{-1}, applied voltage = 12 V).

occur during actual motion of an actuator, one needs to take into accounts various nonlinearities. Among others, geometrical nonlinearity may affect solution accuracy when u_y^A is not small. However, we will consider only linear deformation to simplify the analysis. Furthermore, sequential analyses of electric, thermal and structural phenomena will be used.

The matrix form of the finite element equations for linear electric, heat transfer and structural analysis can be symbolically written as follows (see [8,12,15] for details):

$$\text{Electric problem}: \quad \mathbf{K}_E\mathbf{U}_E = \mathbf{F}_E \tag{1a}$$

$$\text{Heat transfer problem}: \quad \mathbf{K}_T\mathbf{U}_T = \mathbf{F}_T(\mathbf{U}_E) \tag{1b}$$

$$\text{Structural problem}: \quad \mathbf{K}_S\mathbf{U}_S = \mathbf{F}_S(\mathbf{U}_T) \tag{1c}$$

In Eqs. (1a)–(1c), $\mathbf{K}_E$, $\mathbf{K}_T$ and $\mathbf{K}_S$ are stiffness matrices of electrical, heat transfer and structural problems, respectively. The electric field, the temperature, and the structural displacements are denoted by $\mathbf{U}_E$, $\mathbf{U}_T$, and $\mathbf{U}_S$, respectively. In Eqs. (1b) and (1c), $\mathbf{F}_T$ that is a function of $\mathbf{U}_E$ is due to Joule's heat energy and $\mathbf{F}_S$ that is a function of $\mathbf{U}_T$ is due to thermal expansion. In Eqs. (1a)–(1c), thermal and electric conductivities are assumed to be independent of temperature.

To control the minimum length scale during the topology optimization process, the method by [7] is employed. Following the notations in [7], the minimum diagonal length of the solid part of the patch will be defined as $L^{\mathrm{d}}_{\min}$, and the minimum horizontal or vertical length of the solid part of the patch will be defined as $L^{\mathrm{h,v}}_{\min}$. To denote the minimum length scale in the domain discretized by square or rectangular finite elements, the following definition will be used:

$$\mathrm{CT1}\{\text{for all } 2\times 2 \text{ patches } L^{\mathrm{d}}_{\min} \geq \sqrt{2} \quad \text{and} \quad L^{\mathrm{h,v}}_{\min} \geq 1 \tag{2}$$

$$\mathrm{CT2}\begin{cases} \text{for all } 4\times 4 \text{ patches}: L^{\mathrm{d}}_{\min} \geq 2\sqrt{2} \text{ and } L^{\mathrm{h,v}}_{\min} \geq 2 \\ \text{for all } 2\times 2 \text{ patches}: L^{\mathrm{d}}_{\min} \geq \sqrt{2} \text{ and } L^{\mathrm{h,v}}_{\min} \geq 1 \end{cases} \tag{3}$$

$$\mathrm{CT4}\begin{cases} \text{for all } 8\times 8 \text{ patches}: L^{\mathrm{d}}_{\min} \geq 4\sqrt{2} \text{ and } L^{\mathrm{h,v}}_{\min} \geq 4 \\ \text{for all } 4\times 4 \text{ patches}: L^{\mathrm{d}}_{\min} \geq \dfrac{4\sqrt{2}}{2} \text{ and } L^{\mathrm{h,v}}_{\min} \geq \dfrac{4}{2} \\ \text{for all } 2\times 2 \text{ patches}: L^{\mathrm{d}}_{\min} \geq \dfrac{4\sqrt{2}}{4} \text{ and } L^{\mathrm{h,v}}_{\min} \geq \dfrac{4}{4} \end{cases} \tag{4}$$

where 'CT' stands for connection thickness. The concepts of CTn ($n=1$, 2, 4) are briefly described in Table 1. The patch shapes depicted in Table 1 can be realized at the end optimization iterations because all densities for the topology optimization are assumed to be 0 or 1. At the beginning of the topology optimization, CTn ($n=1$, 2, 4) will be selected as the minimum length scale. If the minimum length scale is controlled to be CTn, the hierarchical application of the wavelet shrinkage method [7,16] is used. The hierarchical wavelet shrinkage method is sketched in Fig. 5.

Table 1
The concepts of CT0, CT1, CT2 and CT4 (white pixel: material absence, black pixel: material presence)

Connection thickness	CT0	CT1	CT2	CT4
Patch configuration		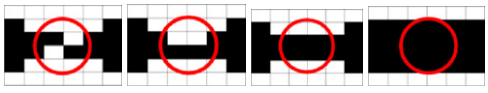		

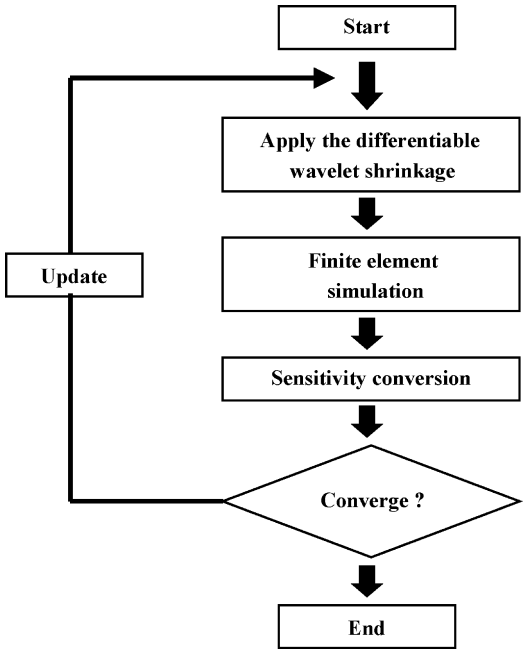

Fig. 5. An overview of the hierarchical wavelet shrinkage method developed to keep structural connections at a minimum.

To solve the problem depicted in Fig. 4, the design domain is discretized by 128×64 finite elements. The mass constraint ratio was 20%. The method of moving asymptotes developed by [17][1] was used as an optimizer for all numerical problems.

The optimized results through topology optimization with the minimum scale length control are shown in Fig. 6. Fig. 7 shows the distributions of the von Mises stresses on the deformed shapes of the optimized results with and without the feature scale control. By examining the nominal V-shape actuator in Fig. 6(a) and the optimized actuators in Fig. 6(b–d), one can see the presence of elastic hinges, i.e., localized narrow necks in all of the optimized results. Because elastic hinges are efficient mechanisms to induce large motion, such hinges are formed by the optimization method. Though the optimized actuator without the minimum length scale control has the largest tip displacement, it has a high stress concentration at its hinges. The length scale controlling algorithm is an indirect way to reduce the maximum-stress level as seen in Fig. 7; because there is no unified technique to control stress level in topology optimization setting, the employed length scale control can be used as a practical alternative. As the width of the hinges increases, Joule's energy becomes less concentrated at the hinges. When CT4 was used, the maximum von Mises stress developed at the hinges became 1/20 of the yield stress. The stress reduction at the sacrifice of the tip displacement increased the yield rate.

[1] The authors appreciate Prof. Svanberg for providing his computer program.

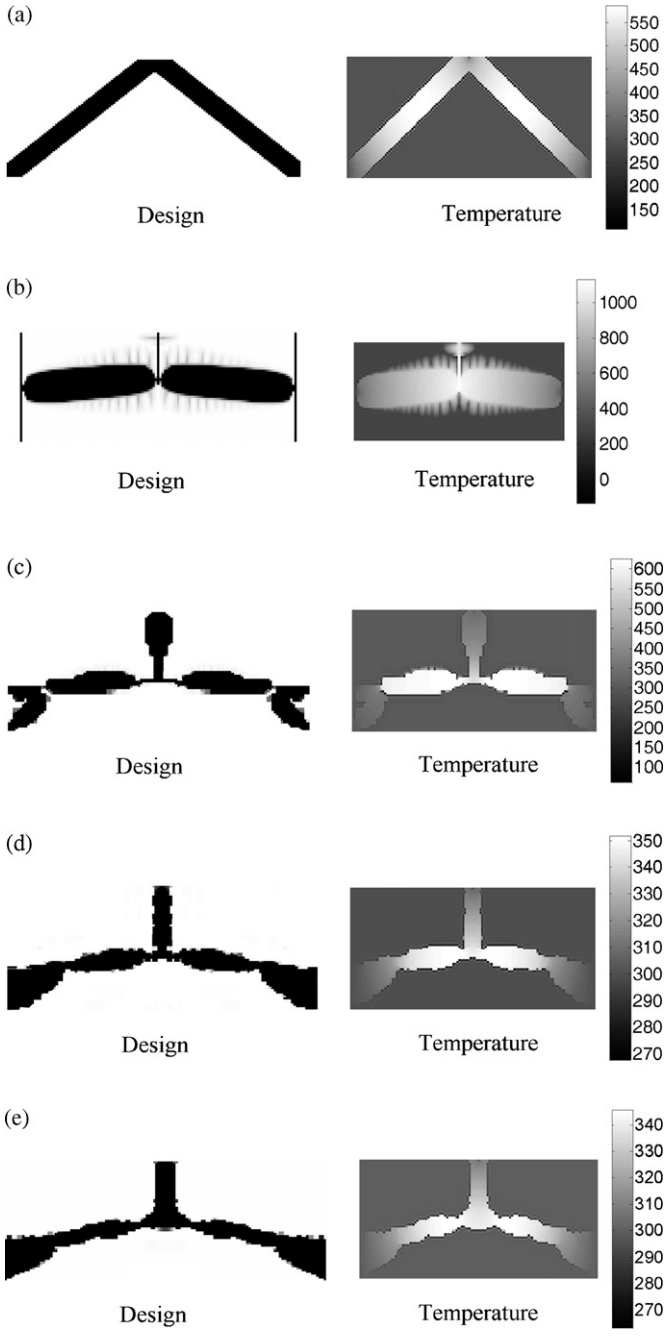

Fig. 6. The optimized results for the thermal actuator design. (a) V-shape design as a reference [18] ($u_y^A = 0.30\,\mu m$), (b) no minimum connection size control ($u_y^A = 3.41\,\mu m$), the minimum connection imposed at (c) CT1 ($u_y^A = 2.86\,\mu m$), (d) CT2 ($u_y^A = 1.58\,\mu m$), (e) CT4 ($u_y^A = 0.99\,\mu m$).

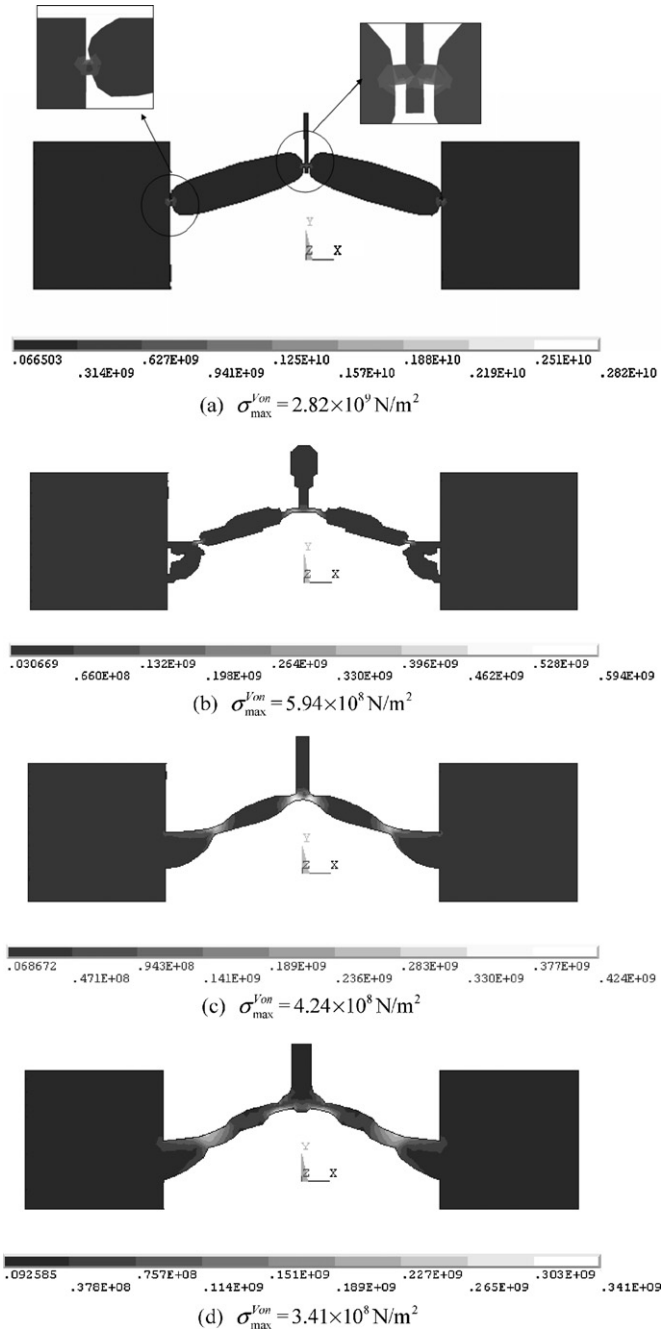

Fig. 7. The von Mises stress distributions on the deformed shapes of the optimized results with (a) no minimum size control, (b) CT1, (c) CT2, and (d) CT2 (yield stress of silicon: $\sigma_{Yield} = 7 \times 10^9\ N/m^2$).

3. Fabrication and experimental results

An SOI wafer was used, whose thicknesses of top silicon, buried oxide, base silicon and resistivity are 15 μm, 3 μm, 525 μm and 0.015 Ω cm, respectively. The fabrication process is shown in Fig. 8. In Fig. 8(b), a 15 μm-thick silicon top is etched using a deep Si etcher to create the shape of actuators. Then, a silicon nitride layer, which is used as a mask for the KOH wet etch, is deposited using a Low Pressure Chemical Vapor Deposition (LPCVD) and the backside silicon is penetrated by KOH as shown in Fig. 8(c). Like Fig. 8(d), the buried oxide is removed by 7:1 BOE (7 parts 40% NH_4F, 1 part 49% HF, Buffered Oxide Etch) and the devices are released. After the silicon nitride is removed, the fabrication process is completed.

For experiment, current was supplied to each of the fabricated actuators. Fig. 1(a) depicts how the input current was applied to a fabricated actuator. The Tungsten tips of a prove station were in contact with the side electrodes. The displacement of an actuator was measured by using the gauge having 50 μm resolutions. High-resolution pictures (190 × 190 pixels

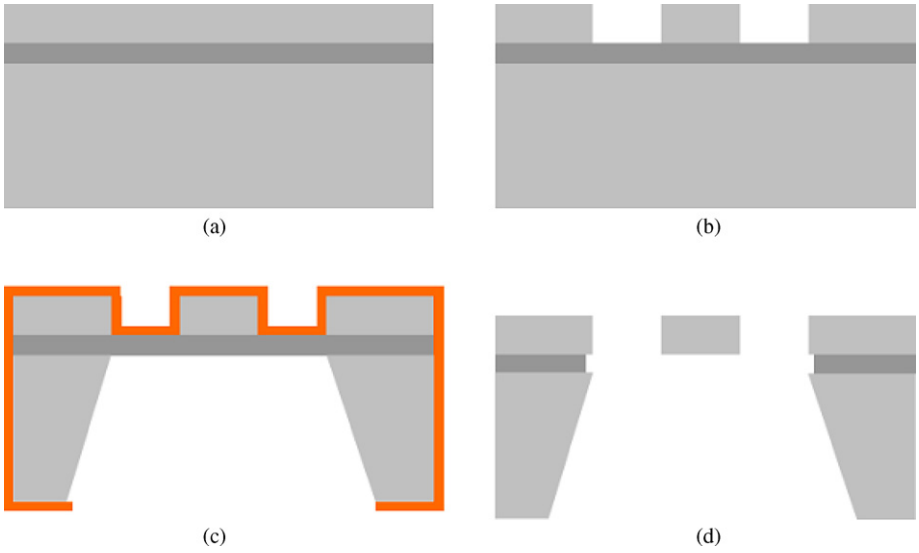

Fig. 8. Fabrication process.

Table 2
Yields comparison of actuators (CT0, CT1, CT2, CT4)

	CT0		CT1		CT2		CT4	
Optimization results	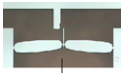				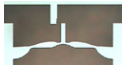		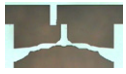	
Thickness of buried oxide (μm)	2	3	2	3	2	3	2	3
No. of success/total no. of trial	13/21	1/21	16/21	3/21	20/21	20/21	21/21	21/21
Yield	62	5	76	14	95	95	100	100

per 100 μm × 100 μm) were taken before and after current was supplied to an actuator. The gauze is shown in the top of Fig. 1(b).

The number of fabricated actuators for each case (CT0, CT1, CT2 and CT4) is 21 and the results are shown in Table 2. The yield rates for CT2 and CT4 are almost 100%, but the yields for CT0 and CT1 are much lower than those for CT2 and CT4. Therefore, devices must be designed with the consideration of the minimum feature size which should be determined by manufacturing conditions.

Table 3 compares the yield rates by Approach 1 and Approach 2. In Approach 1, an optimization is carried out without the minimum length control and the optimized actuator is so post-processed that its minimum length becomes equal to or larger than the prescribed minimum length. In Approach 2, an optimization is carried out with the minimum length controlling scheme. In this case, no post-processing to adjust the minimum length is needed. Approaches 1 and 2 are depicted in Fig. 3.

Let us now check the performance of these actuators or the displacement at A under a given voltage. Table 4 compares the performance of the devices designed by Approaches 1 and 2. When the minimum thickness is 10 μm, the performance by

Table 3
Yield comparison of the actuators with equal minimum thickness

Approach	Picture	Minimum thickness (μm)	No. of success/no. of trial	Yield (%)
1		10	23/32	71
		12	21/33	64
		14	30/32	94
2	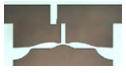	10	32/32	100
		12	33/33	100
		14	32/32	100

Table 4
Performance comparison of the actuators with equal minimum length scale (applied voltage: 12 V)

Approach	Picture	Minimum thickness (μm)	Displacement (μm)	
			Mean	Standard deviation
1		10	0.72	0.47
		12	0.57	0.29
		14	0.47	0.255
2	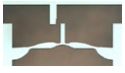	10	0.63	0.16
		12	0.62	0.145
		14	0.60	0.35

Approach 1 is better than that by Approach 2. However, the actuator designed by Approach 2 has better performance than that by Approach 1 when the minimum thickness is 120 μm or 140 μm. Because the maximum measurement error is 0.050 μm (100 μm/190 pixels), the standard deviations in Table 4 can contain relatively large errors. However, the qualitative analysis of Table 4 indicates the relative deviations by Approach 2 are smaller than those by Approach 1.

4. Conclusions

The experiments on micro thermal actuators showed that the optimal topology design method incorporating minimum length scale control considerably improves production yield and reduces actuating performance deviations. For the tested minimum scale, the yield rate from the design optimization method with scale control reached almost 100% while the method without it marked between 71% and 94%. The relative standard deviation in actuation displacement by the method with scale control was smaller than that without the scale control.

Acknowledgements

This research was supported by the National Creative Research Initiatives Program (Korea Science and Technology Foundation Grant Nos. 2006-033 and 2007-019) contracted through the Institute of Advanced Machinery and Design at Seoul National University.

References

[1] S. Schweizer, S. Calmes, M. Laudon, P. Renaud, Thermally-actuated cantilever beam for achieving large in-plane mechanical deflections, Sens. Actuators A 76 (1999) 470–477.
[2] M. Pai, N.C. Tien, Low voltage electrothermal vibromotor for silicon optical bench applications, Sens. Actuators A 83 (2000) 237–243.
[3] J.S. Park, L.L. Chu, A.D. Oliver, Y.B. Gianchandani, Bent-beam electrothermal actuators-Part II: Linear and rotary microengines, J. Microelectromech. Syst. 10 (2) (2001) 255–262.
[4] E.S. Kolesar, M.D. Ruff, W.E. Odom, J.A. Jayachadran, J.B. McAllister, S.Y. Ko, J.T. Howard, P.B. Allen, J.M. Wilken, N.C. Boydston, J.E. Bosch, R.J. Wilks, Single- and double-hot arm asymmetrical polysilicon surface micromachined electro thermal micro actuators applied to realize a microengine, Thin Solid Films 420–442 (2002) 530–538.
[5] H.N. Kwon, S.H. Jeong, S.K. Lee, J.H. Lee, Design and characterization of a micromachined inchworm motor with thermo elastic linkage actuators, Sens. Actuators A 103 (2003) 143–149.
[6] Y. Wang, Z. Li, D.T. McCormick, N.C. Tien, A micromachined RF microrelay with electrothermal actuation, Sens. Actuators A 103 (2003) 231–236.
[7] G.H. Yoon, S. Heo, Y.Y. Kim, Minimum thickness control at various levels for topology optimization using the wavelet method, Int. J. Solid Struct. 42 (2005) 5945–5970.
[8] J. Jonsmann, Technology development for topology optimized thermal microactuators, Ph.D. Thesis, Mikorelektronik Centret, Technical University of Denmark, Denmark, 1999.
[9] M. Elwenspoek, M. Wiegerink, Mechanical Microsensors, Springer-Verlag, New York, 2001.
[10] F. Ayazi, K. Najafi, High aspect-ratio polysilicon micromachining technology, Sens. Actuators A 87 (2002) 46–51.
[11] A. Bertz, M. Kűchler, R. Knőfler, T. Gessner, A novel high aspect ratio technology for MEMS fabrication using standard silicon wafers, Sens. Actuator A 97/98 (2002) 691–701.
[12] O. Sigmund, Design of Multiphysics Actuators using Topology Optimization—Part I: One Material Structure, Comput. Meth. Appl. Mech. Eng. 190 (49/50) (2001) 6577–6604.
[13] Y. Luzhong, G.K. Ananthasuresh, A novel topology design scheme for the multi-physics problems of electro-thermally actuated compliant micromechanisms, Sens. Actuators A 97/98 (2002) 599–609.
[14] S. Park, D. Kwak, H. Ko, T. Song, D. Cho, Selective silicon-on-insulator (SOI) implant: a new micromachining method without footing and residual stress, J. Micromech. Microeng. 15 (2005) 1607–1613.
[15] G.H. Yoon, Y.Y. Kim, The element connectivity parameterization formulation for the topology design optimization of multiphysics systems, Int. J. Numer. Methods Eng. 64 (2005) 1649–1677.
[16] G.H. Yoon, Y.Y. Kim, M.P. Bendsøe, O. Sigmund, Hinge-free topology optimization with embedded translation-invariant differentiable wavelet shrinkage, Struct. Multidisciplinary Optimiz. 27 (3) (2003) 139–150.
[17] K. Svanberg, The method of moving asymptotes—a new method for structural optimization, Int. J. Numer. Methods Eng. 24 (1987) 359–373.
[18] L. Que, J.S. Park, Y.B. Gianchandani, Bent-beam electrothermal actuators—Part I: Single beam and cascaded devices, J. Microelectromech. Syst. 10 (2) (2001) 247–254.